Submitted to the
International Europhysics Conference on High Energy Physics
Aachen, Germany, July 17 – 23, 2003

Abstract: 546 **Plenary Session: 10**
Parallel Session: 5

A Search for the Pion Trajectory in the Photoproduction of Leading Neutrons at HERA

ZEUS Collaboration

15th July 2003

Abstract

Energetic neutrons produced in photoproduction at HERA are studied. These neutrons, carrying a large fraction $x_L > 0.6$ of the incoming proton's beam energy, have small invariant momentum transfer squared $|t| < 0.425$ GeV^2 between the incoming proton and the produced neutron. The x_L distribution of the neutron is measured as a function of t. To a good approximation the $(1 - x_L)$ distribution satisfies a power law $dN/dx_L \propto (1 - x_L)^{a(t)}$ with the powers $a(t)$ lying on a linear trajectory in t: $a(t) = (1.06 \pm 0.06(stat.)^{+0.52}_{-0.42}(syst.)) - (2.78 \pm 0.33(stat.)^{+0.30}_{-0.42}(syst.)\ \mathrm{GeV}^{-2})t$. These values are consistent with the expectation from pion exchange.

1 Introduction

ZEUS has previously reported studies [1–3] of leading neutron production at HERA. In this contribution these analyses are extended for semi-inclusive photoproduction events $\gamma p \to nX$. The kinematic variables t, the invariant momentum transfer squared between the incoming proton and produced neutron, and x_L, the energy fraction of the proton carried by the neutron, are convenient variables for studies energy-angle correlations. This paper studies the $(1-x_L)$ distribution as a function of t for large $x_L > 0.6$ and small $|t| < 0.425$ GeV^2.

2 Description of the experiment

The data used for this measurement were collected at the ep collider HERA with the ZEUS detector during the year 2000, when HERA collided 27.5 GeV positrons with 920 GeV protons, giving a center-of-mass energy of 318 GeV. The integrated luminosity of the used sample is 9 pb^{-1}.

For photoproduction events used in this analysis the small angle scattered electron was measured with the LUMI calorimeter, a lead-scintillator calorimeter [4] located at $Z = -35$ m.

The forward neutron calorimeter (FNC) [5–7] was installed in the HERA tunnel at $\theta = 0$ degrees and at $Z = 106$ m from the interaction point in the proton-beam direction, and used for the 1995-2000 data taking. Magnet apertures limit the FNC acceptance to neutrons with production angles less than 0.8 mrad, giving transverse momenta $p_T \leq E_n\theta_{\text{max}} = 0.74x_L$ GeV. The FNC is a lead-scintillator calorimeter with an energy resolution for hadrons of $\sigma_E/E = 0.70/\sqrt{E(\text{GeV})}$. Three planes of veto counters were located in front of the FNC.

In the spring of 1998 a forward neutron tracker (FNT) was installed in the FNC at a depth of one interaction length. It is a hodoscope designed to measure the position of neutron showers and consists of scintillator fingers, 17 for X position reconstruction and 15 for Y. Each scintillator finger is 16.8 cm long, 1.1 cm wide and 0.5 cm deep. Figure 1 shows the position of the FNT hodoscope in the FNC relative to the incoming neutron beam. The irregular outlined area shows the geometric acceptance. Scans by a radioactive ^{60}Co source were performed to calibrate and monitor both detectors.

The position resolution of neutron showers in the FNT was measured by placing an adjustable collimator in front of the outermost veto counter of the FNC during special test and calibration runs. The measured position resolution was ± 0.26 cm.

3 Kinematics and Event Selection

The kinematics of tagged photoproduction $ep \to eX$ at HERA is specified by the photon-proton center-of-mass energy, W which is related to the electron-proton center of mass energy, $\sqrt{s}$, and by $W^2 = ys$ where y is the inelasticity of the electron, $y = (E - E')/E$ and $E(E')$ is the energy of the incoming(scattered) electron.

For the semi-inclusive process $ep \to enX$ additional variables are used: the energy E_n and the production angle θ_n of produced neutron. The energy is given in terms of $x_L = E_n/E_p$ where E_p is the energy of the incoming proton beam. These variables are related to the transverse momentum of the neutron by $p_T = E_n\theta_n$ and to the invariant momentum transfer squared t between the incoming proton and the neutron by

$$t = -\frac{p_T^2}{x_L} - \frac{(1-x_L)}{x_L}\left(m_n^2 - x_L m_p^2\right)$$

where m_p is the mass of the proton and m_n is the mass of the produced neutron.

The neutron energy was reconstructed using the FNC and the neutron production angle using the FNT. The inelasticity y was reconstructed using the LUMI electron calorimeter.

Photoproduction events were selected using cuts based on the reconstructed vertex position of the interaction point and calorimeter energy deposits. The events were required to have an energy in the LUMI electron calorimeter satisfying $10 < E_e < 18$ GeV. These cuts restrict the range of of the virtuality of the exchanged photon Q^2 to be less than ~ 0.02 GeV^2, with a median value of $\approx 10^{-3}$ GeV^2, which is small compared to W^2.

Events with a leading neutron were selected by requiring a large energy deposit ($x_L > 0.2$) in the FNC. The events with an energy deposition consistent with a proton, photon or neutrons starting a shower in front of the FNC were removed [3].

Further, events were required to have an energy deposit in the FNT and to satisfy the criterion that the fingers with the most deposited energy and the second most deposited energy be adjacent. The FNT cuts reduced the sample to 24k events.

4 Neutron Efficiencies and Correction Factors

The efficiencies and correction factors for the produced neutron were calculated using samples of Monte Carlo simulation events. The ZEUS detector response to generated particles, including the proton beam-line elements, absorbing material, proton beam spread, and the measured resolutions of the FNC and FNT for incident neutrons was simulated in detail. Monte Carlo events were generated to match the observed uncorrected distributions and the corrected distributions obtained using bin-by-bin unfolding [2]. The trigger efficiency of the FNC was close to 100% for the energy range under consideration here ($x_L > 0.6$) and can be neglected.

5 Systematic uncertainties

The main systematic effects were:

- the uncertainty in the absolute energy scale of the FNC of $\pm 3\%$;
- the uncertainty in the position of the beam spot: $(\Delta X, \Delta Y) = (\pm 0.1, \pm 0.1)$ cm;
- the uncertainty in the simulation of absorbing material obtained from direct measurements of the proton beam line: the absorbing material was mapped using low energy ($0.16 < x_L < 0.27$) neutron data. An independent analysis was made using this absorbing material map and its results are comparable to those obtained from the direct measurements of the proton beam line.

6 Results

The x_L distribution of neutrons for photoproduction, $\gamma p \rightarrow nX$, in bins of t are shown in Fig. 2. The error bars show the contribution of the statistical error to the total uncertainty. The distributions follow approximate power laws in $(1 - x_L)$ with $dN/dx_L \propto (1 - x_L)^{a(t)}$. For each t value the power $a(t)$ was obtained by a least squared fit to the observed distribution for $x_L < 0.925$. Only statistical errors were used in the fits because the systematic uncertainties are highly correlated point to point. The resulting fits are superimposed on the measured data points.

The powers are plotted as a function of $-t$ in Fig. 3. The inner error bars show the statistical contribution to the total uncertainty. The powers are describing a linear trajectory in t:

$$a(t) = (1.06 \pm 0.08(stat.)^{+0.52}_{-0.42}(syst.)) - (2.78 \pm 0.33(stat.)^{+0.30}_{-0.42}(syst.)\ \mathrm{GeV}^{-2})t$$

The uncertainties in the intercept I and the slope S are correlated by $\delta I/\delta S \cong -0.65$.

7 Discussion

Previous experiments have shown that leading neutron production in lepton-hadron interactions is well described by pion exchange models [2, 3, 8]. It is possible to test this directly by assuming pion exchange is the correct mechanism and deriving the pion trajectory from the measured value of $a(t)$, as follows. The pion "flux", the splitting function of a proton to a neutron and pion ($p \to n\pi^+$), can be parameterized as (see [2] and the references cited therein):

$$f_{\pi/p}(x_L, t) = \frac{1}{4\pi}\frac{g^2_{n\pi p}}{4\pi}\frac{-t}{(m^2_\pi - t)^2}(1 - x_L)^{1-2\alpha_\pi(t)}\,(F(t))^2$$

where $g_{n\pi p}$ is the coupling at the $n\pi p$ vertex, m_π is the mass of the pion, and $\alpha_\pi(t) = \alpha'_\pi t$ is the Regge trajectory (with slope α'_π and intercept $\mathcal{O}(m^2_\pi)$) of the pion. $F(t)$ is a form-factor which accounts for final state rescattering of the neutron. If F does not depend on x_L then the flux is of the form $f_{\pi/p} = A(t)\,(1 - x_L)^{a(t)}$, where the normalization A and the power a are functions of t. The cross section for neutron production is given by a convolution of the flux and the total $\gamma\pi \to X$ cross section $\sigma_{\gamma\pi} = \sigma_{\gamma\pi}(s')$:

$$\frac{d^2\sigma}{dx_L dt} = A(t)(1 - x_L)^{a(t)}\sigma_{\gamma\pi}\left((1 - x_L)W^2\right)$$

where $s' = (1 - x_L)W^2$ is the $\gamma\pi$ cm energy. For photoproduction $\sigma_{\gamma\pi}$ has a power law dependence on s' for large s' of the Donnachie-Landshoff form [9]

$$\sigma_{\gamma\pi}(s') = \mathcal{A}(s')^\epsilon + \mathcal{B}(s')^{-\eta}$$

where $\epsilon \approx 0.1$ and $\eta \approx 0.5$. For large s' the Pomeron $I\!P$ (ϵ) dominates the Reggeon $I\!R$ (η). In this case the $(1 - x_L)$ distribution is proportional to $(1 - x_L)^{a_{eff}(t)}$ where the effective power is given by

$$a_{eff}(t) = 1 + \epsilon - 2\alpha'_\pi t.$$

The experimental result is:

$$1 + \epsilon = \alpha_{I\!P}(0) = 1.06 \pm 0.08(stat.)^{+0.52}_{-0.42}(syst.)$$

and

$$\alpha'_\pi = 1.39 \pm 0.17(stat.)^{+0.15}_{-0.21}(syst.)\,\mathrm{GeV}^{-2}$$

These measured values are consistent, within errors, with the expectation of $\alpha_{I\!P}(0) \simeq 1.1$ and $\alpha'_\pi \simeq 1$ and so give direct evidence for the dominance of pion exchange in this reaction.

Conclusions

It is found that to a good approximation the $(1 - x_L)$ distribution in the process $\gamma p \to nX$ satisfies a power law $dN/dx_L \propto (1 - x_L)^{a(t)}$ with the powers $a(t)$ lying on a linear trajectory in t. The measured values of the intercept and the slope are in agreement with expectations from pion exchange.

Acknowledgments

We thank the DESY Directorate for their strong support and encouragement, and the HERA machine group for their diligent efforts. We are grateful for the support of the DESY computing and network services. The design, construction and installation of the ZEUS detector have been made possible owing to the ingenuity and effort of many people from DESY and home institutes who are not listed as authors.

References

[1] ZEUS Coll., M. Derrick et al., Phys. Lett. **B 384**, 388 (1995).

[2] ZEUS Coll., J. Breitweg et al., Nucl. Phys. **B 596**, 3 (2000).

[3] ZEUS Coll., J. Breitweg et al., Nucl. Phys. **B 637**, 3 (2002).

[4] J. Andruszków et al., Preprint DESY-92-066, DESY, 1992;
ZEUS Coll., M. Derrick et al., Z. Phys. **C 63**, 391 (1994);
J. Andruszków et al., Acta Phys. Pol. **B 32**, 2025 (2001).

[5] ZEUS FNC group, S. Bhadra et al., Nucl. Inst. Meth. **A 354**, 479 (1995).

[6] ZEUS FNC group, S. Bhadra et al., Nucl. Inst. Meth. **A 394**, 121 (1997).

[7] ZEUS FNC Group, S. Bhadra et al., *Proc. of the Seventh International Conference on calorimetry in High Energy Physics, Tuscon, Arizona, November 1997*, E. Cheu et al. (ed.), p. 295. World Scientific, Singapore (1998).

[8] H1 Coll., C. Adloff et al., Eur. Phys. J. **C 6**, 587 (1999).

[9] A. Donnachie and P.V. Landshoff, Phys. Lett. **B 296**, 227 (1992).

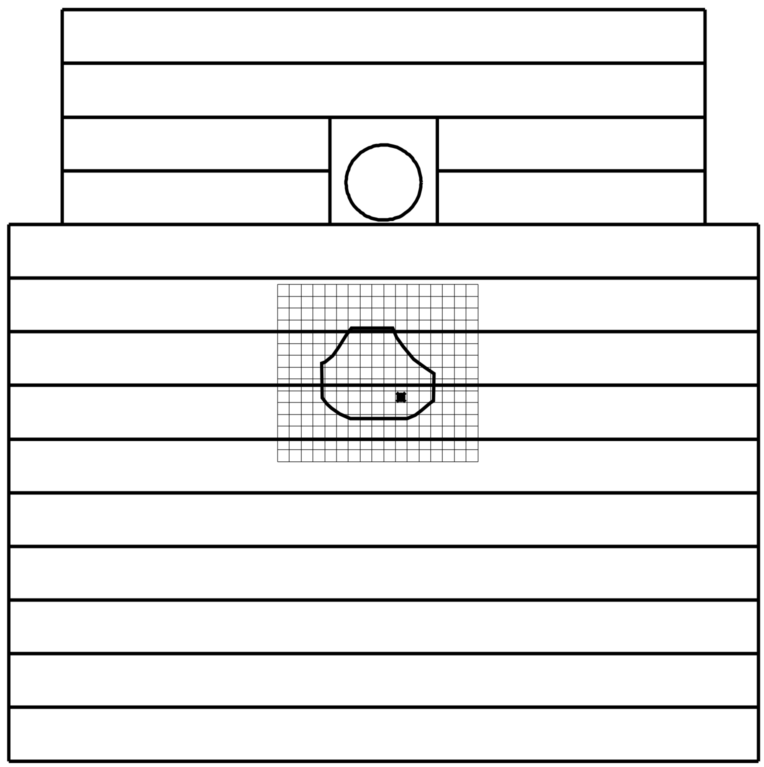

Figure 1: *The FNC as viewed from the front, showing the 14 towers in which the calorimeter is segmented. The FNT hodoscope and its scintillator fingers are also shown, superimposed by a curve outlining the geometric acceptance allowed by the proton beam line elements. The black dot shows the position of the projection of the beam spot.*

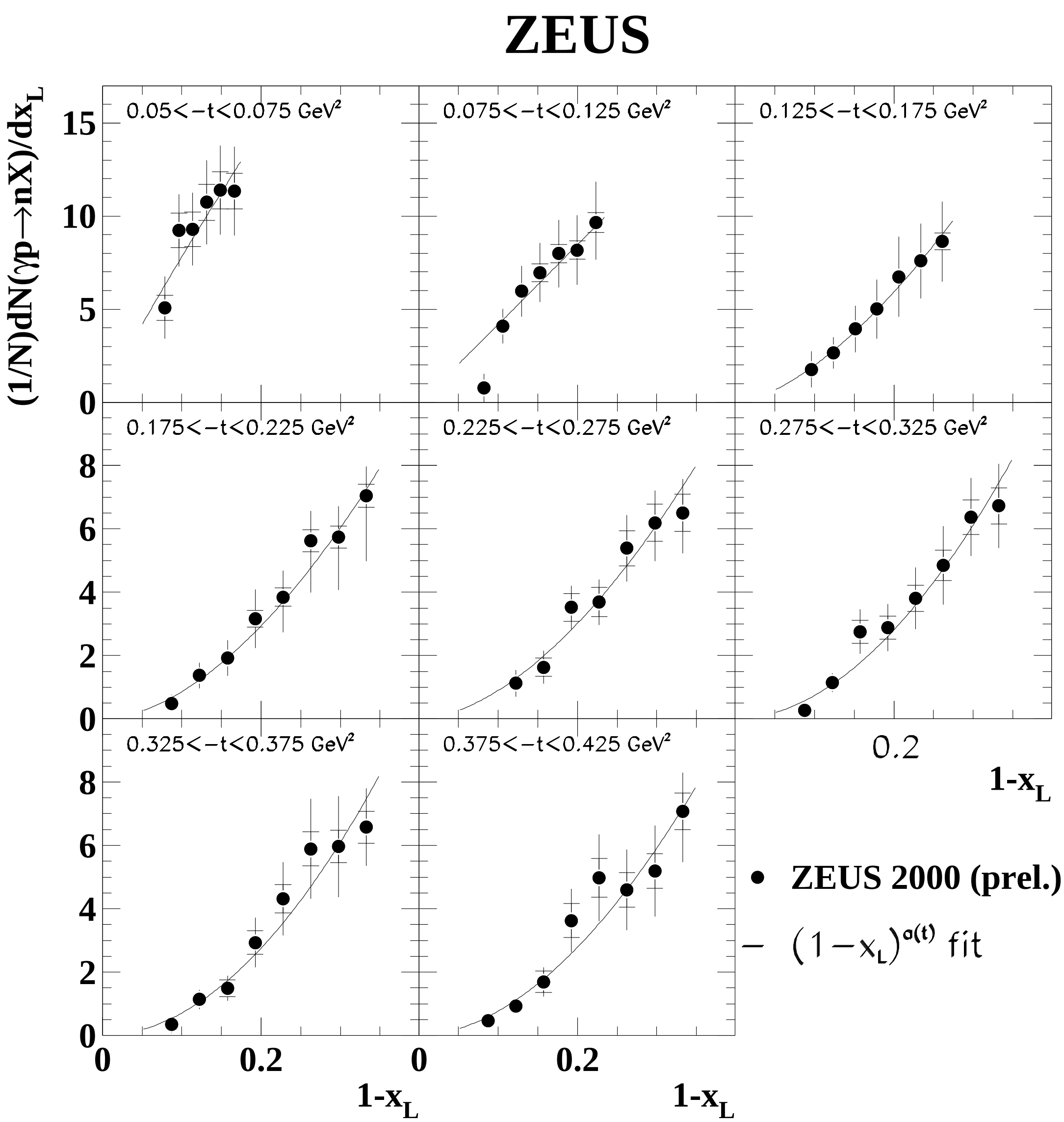

Figure 2: *The neutron x_L distribution for semi-inclusive photoproduction, $\gamma p \to nX$, in bins of invariant momentum transfer squared t. The curves show the results of fits to the data with $x_L < 0.95$ of the form $\propto (1 - x_L)^{a(t)}$. The error bars show the contribution of statistical error to the total uncertainty. Only statistical errors are used in the fits.*

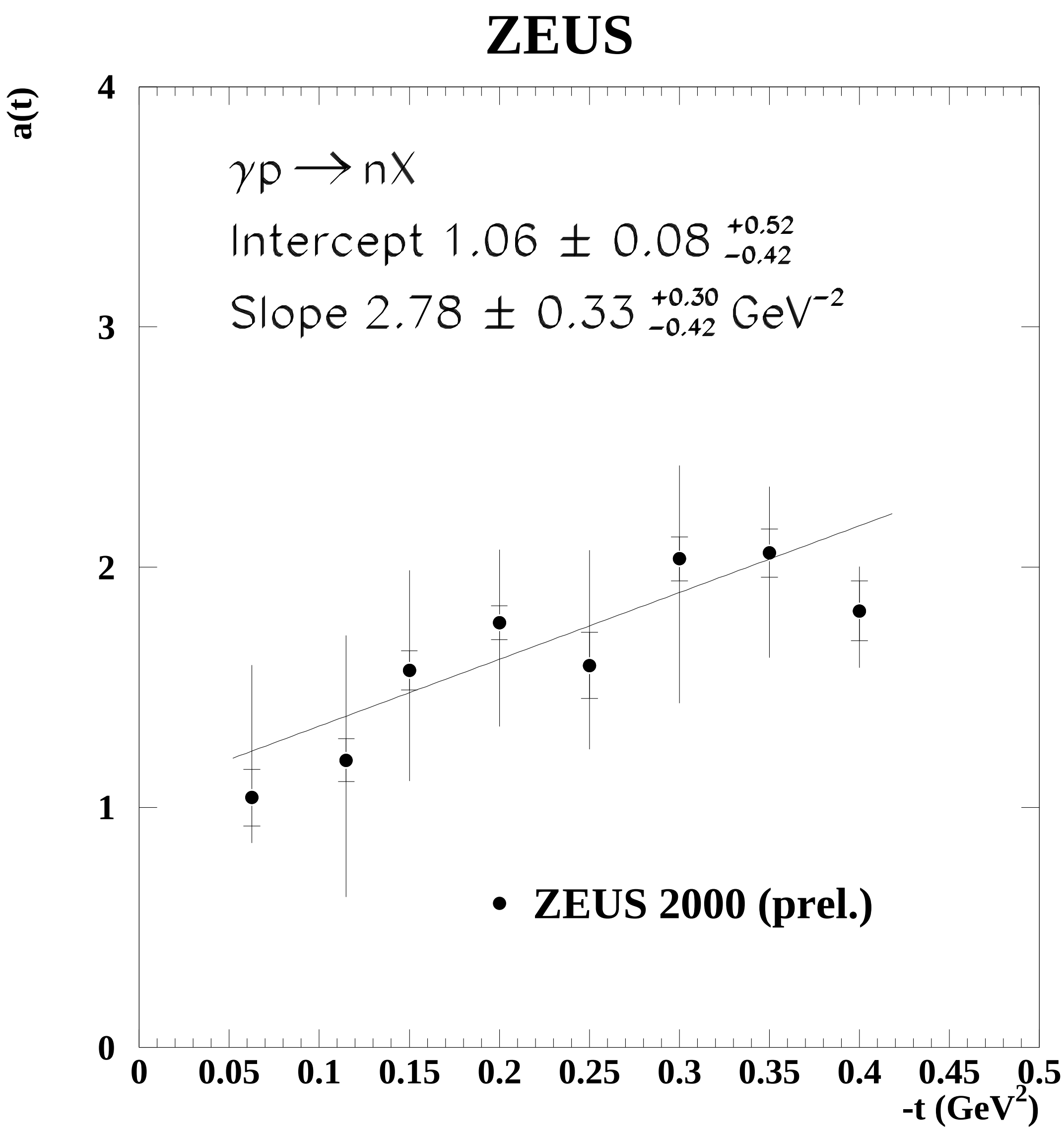

Figure 3: *The powers determined by least squared fits to the $1 - x_L$ distributions in semi-inclusive photoproduction, $\gamma p \rightarrow nX$, as a function of the invariant momentum transfer squared t. The powers form a trajectory in t which has been fit to a straight line. The inner error bars show the contribution of statistical error to the total uncertainty. Only statistical errors are used in the fit.*